Title

REH2C Helicase and GRBC Subcomplexes May Base Pair through mRNA and Small Guide RNA in Kinetoplastid Editosomes*

Journal

Journal of Biological Chemistry, 291(11)

ISSN

0021-9258

Authors

Kumar, Vikas
Madina, Bhaskara R
Gulati, Shelly
et al.

Publication Date

2016-03-01

DOI

10.1074/jbc.m115.708164

Peer reviewed

THE JOURNAL OF BIOLOGICAL CHEMISTRY VOL. 291, NO. 11, pp. 5753–5764, March 11, 2016

REH2C Helicase and GRBC Subcomplexes May Base Pair through mRNA and Small Guide RNA in Kinetoplastid Editosomes*

Received for publication, December 3, 2015, and in revised form, January 5, 2016 Published, JBC Papers in Press, January 14, 2016, DOI 10.1074/jbc.M115.708164

Vikas Kumar[‡1], Bhaskara R. Madina[‡1,2], Shelly Gulati[§], Ajay A. Vashisht[¶], Chiedza Kanyumbu[§], Brittany Pieters[‡], Afzal Shakir[§], James A. Wohlschlegel[¶], Laurie K. Read[‖], Blaine H. M. Mooers[§], and Jorge Cruz-Reyes[‡3]

From the [‡]Department of Biochemistry and Biophysics, Texas A&M University, College Station, Texas 77843, the [¶]Department of Biological Chemistry, David Geffen School of Medicine, University of California, Los Angeles, Los Angeles, California 90095, the [‖]Department of Microbiology and Immunology, University of Buffalo School of Medicine, Buffalo, New York, and the [§]Department of Biochemistry and Molecular Biology, University of Oklahoma Health Sciences Center, Oklahoma City, Oklahoma 73104

Mitochondrial mRNAs in *Trypanosoma brucei* undergo extensive insertion and deletion of uridylates that are catalyzed by the RNA editing core complex (RECC) and directed by hundreds of small guide RNAs (gRNAs) that base pair with mRNA. RECC is largely RNA-free, and accessory mitochondrial RNA-binding complex 1 (MRB1) variants serve as scaffolds for the assembly of mRNA-gRNA hybrids and RECC. However, the molecular steps that create higher-order holoenzymes ("editosomes") are unknown. Previously, we identified an RNA editing helicase 2-associated subcomplex (REH2C) and showed that REH2 binds RNA. Here we showed that REH2C is an mRNA-associated ribonucleoprotein (mRNP) subcomplex with editing substrates, intermediates, and products. We isolated this mRNP from mitochondria lacking gRNA-bound RNP (gRNP) subcomplexes and identified REH2-associated cofactors 1 and 2 (^{H2}F1 and ^{H2}F2). ^{H2}F1 is an octa-zinc finger protein required for mRNP-gRNP docking, pre-mRNA and RECC loading, and RNP formation with a short synthetic RNA duplex. REH2 and other eukaryotic DEAH/RHA-type helicases share a conserved regulatory C-terminal domain cluster that includes an oligonucleotide-binding fold. Recombinant REH2 and ^{H2}F1 constructs associate in a purified complex *in vitro*. We propose a model of stepwise editosome assembly that entails controlled docking of mRNP and gRNP modules via specific base pairing between their respective mRNA and gRNA cargo and regulatory REH2 and ^{H2}F1 subunits of the novel mRNP that may control specificity checkpoints in the editing pathway.

RNA editing by uridylate insertion and deletion in *Trypanosoma brucei* modifies over 3000 sites in mitochondrial mRNAs in a gradual process directed by hundreds of small guide RNAs (gRNAs)[4] (1–3). The basic regulatory mechanisms of substrate specificity and developmental control in RNA editing remain unknown. The uridylate changes are catalyzed by the RECC enzyme from 3′ to 5′ in discrete blocks. Each gRNA directs editing of one mRNA block. Surprisingly, RECC has little or no RNA and lacks the processivity found *in vivo*, as established in early purifications of this multiprotein enzyme (4–6). So, accessory components of the editing apparatus must facilitate substrate recruitment and editing catalysis. There are many non-RECC proteins that affect editing. Most of these proteins (>25 proteins) are components of the MRB1 complex in *T. brucei*, also termed gRNA-binding complex (GRBC) in *Leishmania*, that binds and stabilizes gRNA. MRB1 interacts transiently with the RECC enzyme and mitoribosomes (1, 7, 8). It has also been found that MRB1 contains all three classes of mRNA in editing: unedited pre-mRNAs, partially edited intermediates, and fully edited transcripts. This indicates that MRB1 complexes serve as scaffolds for the assembly of hybrid substrates and the RECC enzyme (9–11). Transient addition of RECC to these scaffolds would establish higher-order editing holoenzymes or editosomes. MRB1 was first considered a single dynamic complex, but the reason of its variable composition was unclear. However, layers of organization in MRB1 are emerging. We found MRB1 variants or MRBs (REH2-MRB and 3010-MRB) via immunoprecipitation (IP) of RNA-editing helicase 2 (REH2) and MRB3010 (3010), respectively. These complexes have REH2 or 3010 but not both and differ in the content of some initiating gRNAs, according to Western blotting and deep sequencing analyses, respectively (9). Recent studies and this work show that these MRBs consist of several subcomplexes (summarized in Fig. 1) (10, 11). 3010-MRB includes GRBC, also called MRB1 core (12). REH2-MRB includes the

* This work was supported by National Science Foundation Grant NSF1122109 (to J. C. R.), NIAID/National Institutes of Health Grant R01 AI088011 (to B. H. H. M.), a NIGMS/National Institutes of Health institutional development award under Grant P20 GM103640 (Principal Investigator, Ann West), NIGMS/National Institutes of Health Grant RO1 GM089778 (to J. A. W.), and NIAID/National Institutes of Health Grant RO1 AI061580 (to L. K. R.). The authors declare that they have no conflicts of interest with the contents of this article. The content is solely the responsibility of the authors and does not necessarily represent the official views of the National Institutes of Health.

[1] Both authors contributed equally to this work.

[2] Present address: Dept. of Veterinary and Animal Sciences, University of Massachusetts, Amherst, MA 01003.

[3] To whom correspondence should be addressed: Dept. of Biochemistry and Biophysics, Texas A&M University and Texas AgriLife Research, 2128 TAMU, College Station, TX 77843. Tel.: 979-458-3374; Fax: 979-845-4059; E-mail: cruzrey@tamu.edu.

[4] The abbreviations used are: gRNA, guide RNA; RECC, RNA editing core complex; GRBC, guide RNA-binding complex; MRB, mitochondrial RNA-binding; IP, immunoprecipitation; mRNP, mRNA-associated ribonucleoprotein; CTD, C-terminal domain cluster; OB, oligonucleotide-binding domain; qRT-PCR, quantitative PCR; dsRBD, double-stranded RNA-binding domain; TEV, tobacco etch virus; dsRNA, double-stranded RNA; Znf, zinc finger; mtRNA, mitochondrial RNA; REMC, RNA editing mediator complex; RESC, RNA editing substrate binding complex.

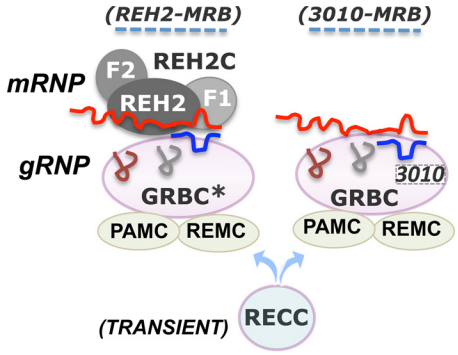

FIGURE 1. **RNP subcomplexes with mRNA (*mRNP*) or gRNA (*gRNP*) in MRB1.** Two stable forms of the MRB1 complex (termed MRBs) are known. Each MRB form consists of multiple subcomplexes. In this study, we characterize the REH2C subcomplex (with its protein subunits indicated as *gray ovals*). This subcomplex includes the REH2 helicase, two cofactors (^{H2}F1 and ^{H2}F2), and mRNA (pre-edited partially edited, and edited). GRBC* and GRBC are variants of another subcomplex that contains gRNAs and several proteins. These gRNA-bound variants are distinguished by their content of a protein subunit (3010). Only GRBC* binds REH2C via stable RNA contacts. Two more subcomplexes, REMC and the polyadenylation mediator complex (*PAMC*), participate in RNA editing and post-editing mRNA 3′ maturation, respectively. Holo-editosomes are formed upon transient addition of the RECC enzyme to the higher-order complexes. The initiating gRNA hybridizes to the 3′ most block in the pre-edited mRNA. The mRNAs are shown in *red*, and the gRNA transcripts are shown in various colors.

REH2 subcomplex (REH2C) and a variant of GRBC (11). To distinguish these gRNA-bound variants, hereafter we refer to GRBC and GRBC*, found in IPs of 3010 and REH2, respectively. GRBC and GRBC* bind multiple gRNAs (9). Other proposed subcomplexes of MRBs are REMC (typified by RGG2) and the polyadenylation mediator complex. These subcomplexes take part in editing progression and post-editing mRNA 3′ maturation, respectively (13, 14).

As the physical organization of MRBs becomes clearer, specialized subcomplexes and critical domains in their subunits open a path to study editing control in substrate-bound molecular scaffolds. For example, the stable association of REH2 with mRNA and GRBC* requires the functional domains in the helicase for dsRNA binding and ATP binding/hydrolysis (11, 15). Also, REH2 helicase is a *trans* factor that promotes pre-mRNA association and editing progression in the 3010-MRB variant (11). Our reported findings represent the first identified *cis* and *trans* effects by the sole MRB1 protein with RNA helicase conservation in editosome assembly and function (11, 15). This study provides new insights into the assembly and regulation of higher-order editosomes, with REH2C playing a central role. REH2C is an mRNA-associated ribonucleoprotein subcomplex (mRNP) that includes REH2, two cofactors (^{H2}F1 and ^{H2}F2), and all mRNA types in editing: pre-mRNA substrates, partially edited transcripts, and fully edited products. The integrity of this mRNP is independent of the GRBC variants. We propose that assembly of stable mRNA-gRNA hybrids in editing scaffolds requires docking of mRNP and gRNP modules by base pairing of mRNA and gRNA. The helicase mRNP binds stably with GRBC* but interacts with GRBC via transient contacts.

Our homology modeling of REH2 revealed a conserved regulatory C-terminal domain cluster (CTD) in eukaryotic RHA-type helicases. This CTD includes winged helix, ratchet, and oligonucleotide-binding (OB) fold domains. ^{H2}F1 has eight putative Cys^2His^2 zinc fingers potentially involved in dsRNA or protein binding. ^{H2}F2 has a glycine-rich C terminus. ^{H2}F1 depletion caused *cis* and *trans* effects. That is, ^{H2}F1 promotes GRBC* association with REH2, RECC, and pre-mRNA (in *cis*) and GRBC association with RECC and pre-mRNA (in *trans*). ^{H2}F1 depletion had no major effect on REH2-dependent unwinding of a synthetic short RNA duplex. However, it inhibited RNP formation with this RNA duplex in *cis* and in *trans*. Purified recombinant REH2 and ^{H2}F1 form a complex *in vitro*. The regulatory REH2 helicase and its eight-zinc finger ^{H2}F1 cofactor enable studies of mRNA-gRNA hybrid assembly and substrate access to RECC on molecular scaffolds. This stepwise process creates the catalytic center in editosomes and likely entails specificity checkpoints.

Experimental Procedures

Cell Culture—T. brucei Lister strain 427 29-13 procyclic "PF" was grown axenically in log phase in SDM79 medium (16) and harvested at a cell density of 1–3 × 10^7 cells/ml. Cell lines expressing constructs for RNAi-based genetic down-regulation were induced with tetracycline at 1 μg/ml.

DNA Constructs—We made inducible RNAi constructs for ^{H2}F1 and GAP1 as described previously (17, 18). The RNAi construct for REH2 has been reported in our previous study (15). RNAi and TAP-tagged constructs for ^{H2}F2 were both prepared by PCR amplification of an 804-bp fragment from the ^{H2}F2 entire open reading frame using 5′-CTCGAGATGTTCCGCTGGTCG-3′ and 5′-AGATCTGGTTAAGGACGCAGAAAC-3′ as forward and reverse primers, respectively. The amplified fragments were cloned into the XhoI and BamHI sites of p2T7-177 or pLEW79-TAP (15, 19). All constructs were confirmed by DNA sequencing, linearized with NotI, and transfected in procyclic 29-13 trypanosomes (16).

Protein and RNA Sample Purification—Immunoprecipitation of REH2, MRB3010 (3010), and cytochrome oxidase 2 (mock) from freshly made mitochondrial extracts was performed using affinity-purified peptide antibodies as described previously (9). Affinity-purified antibodies against ^{H2}F1 and ^{H2}F2 were produced (Bethyl Laboratories, Inc.) in rabbits using the peptides CKRKKTTEVSEVTS and KVSAESYVDYLQNSDRELPA as antigens, respectively. As in our previous studies (9, 11), specific antibodies were conjugated to Dynabeads protein A (Life Technologies) pretreated with 5% BSA. Approximately 2 mg of mitochondrial extract was supplemented with 1× complete protease inhibitor mixture (Roche) and SUPERase In RNase inhibitor (Life Technologies). The extract was precleared by passage over protein A-Sepharose beads (GE Healthcare) before it was loaded onto antibody-conjugated beads. All washes were performed with 200 mM NaCl, 1 mM EDTA, 10 mM $MgCl_2$, and 25 mM Tris (pH 8). Protein was extracted with 1× SDS loading buffer at 95 °C for 2 min. RNA was extracted by treating the beads with 0.8 units of proteinase K (New England Biolabs) for 30 min at 55 °C, followed by phenol extraction and ethanol precipitation. For mass spectrometry analyses, the antibodies were cross-linked to the beads with 25 mM dimethylpimelimidate in 0.2 M triethanolamine (pH 8.2). Samples from tandem affinity-purified complexes were prepared for protein identification as in prior studies (15, 20).

Mass Spectrometry—The immunopurified or tandem affinity-purified protein complexes were reduced, alkylated, and digested as described previously (21, 22). The peptide mixture was desalted, concentrated using C18-packed pipette tips (Thermo Fisher), and fractionated online using a 75 μm inner diameter fitted fused silica capillary column with a 5 μM pulled electrospray tip and packed in-house with 17 cm of Luna C18(2) 3 μM reverse-phase particles. The gradient was delivered via an easy-nLC 1000 ultra high pressure liquid chromatography system (Thermo Fisher). MS/MS spectra were collected on a Q-Exactive mass spectrometer (Thermo Fisher) (23, 24). Data analysis was performed with ProLuCID and DTASelect2 implemented in the Integrated Proteomics Pipeline (IP2, Integrated Proteomics Applications, Inc., San Diego, CA) (25–28). Protein and peptide identifications were filtered with DTASelect and required at least two unique peptides per protein with a peptide-level false positive rate of 5%, as estimated by a decoy database approach (29). Normalized spectral abundance factor values were calculated as described previously (30) and multiplied by a factor of 10^5 for readability.

Western Blotting and Radioactivity Assays—Western blotting analyses of REH2, 3010, GAP1, RGG2, and KREPA1 (also termed MP81, a RECC core subunit) were performed as reported previously (13, 15, 31). Western blotting of MRB6070 and MRB8170 was performed as in Ref. 12 (data not shown). Western blotting of ^{H2}F1 and ^{H2}F2 was performed with sera diluted to 1:2000. RNA ligases in the RECC enzyme were radioactive by self-adenylation directly on the beads (32). Capping assays of gRNA used RNA extracted from the Dynabeads protein A pulldowns (15). Unwinding assays of REH2 or ^{H2}F1 antibody pulldowns were performed as in our previous studies, with a few modifications (15, 33). The RNA duplex substrate in the assays in this study was prepared by annealing 5′GUCUUACGGUGUCUAAAACAAAACAAAACAAAACAAAG3′ (38 nt) and complementary 5′GACACCGUAAGAC3′ (13 nt). 5 pmol of 38-nt oligonucleotide and 0.5 pmol of 5′-labeled 13-nt oligonucleotides were boiled at 95 °C for 2 min, followed by preannealing for 30 min at room temperature in 10× annealing buffer (100 mM MOPS, 10 mM EDTA (pH 6.5), and 0.5 M KCl), and then the hybrids were isolated from a native acrylamide gel run in the cold room at 50 V for 120 min (0.5× Tris borate-EDTA buffer). After the IPs, 20 counts per second of hybrid was mixed with antibody-conjugated beads (5 μl of resin) and incubated for 30 min at 19 °C in 40 mM Tris-Cl (pH 8.0), 0.5 mM $MgCl_2$, 0.01% Nonidet P-40, and 2 mM DTT. The reaction was stopped by addition of 5 μl of helicase reaction stop buffer (2× helicase reaction stop buffer contained 50 mM EDTA, 1% SDS, 0.1% bromphenol blue, 0.1% xylene cyanol, and 20% glycerol) and kept on ice for 5 min. The beads were then collected in a magnetic stand, and the released complexes in solution were loaded onto the native gel and resolved at 25 V, 4 °C for 120 min.

Quantitative RT-PCR of mRNAs and Densitometry—RNA from total mtRNA or pulldowns was treated with RNase-free DNase (Thermo) and used in the preparation of cDNA as described elsewhere (9). qRT-PCR assays normalized using the "ΔΔCq" (Livak) method (34, 35) were performed in 20-μl reactions with primers reported to be specific for unedited mRNAs, fully edited mRNA, and reference transcripts (35) in a SYBR Green PCR Master Mix (Bio-Rad). The editing phenotype in total mtRNA was analyzed as in prior studies (11) using two biologically distinct samples under similar induction conditions (days 3 and 4, in lieu of identical biological replicates). Measurements were normalized to uninduced cells (set at 1) and to tubulin and 18S rRNA references. -Fold change determinations of bound mRNAs in purified complexes from RNAi cells, as in a prior study (11), were made on the basis of the ratio of each mRNA in the IPs and total mtRNA input on days 3 and 4 of induction. The ratio in induced samples was plotted relative to the ratio in uninduced samples (day 0 set at 1). qRT-PCR calculations were normalized to a mock IP and input values. As in the phenotypic analyses, two biologically distinct samples under similar induction conditions (days 3 and 4) were examined in parallel measurements. In all analyses, two technical replicates were obtained per Cq measurement. The maximum standard deviation of the average value in the Cq duplicates that was observed in the entire analysis is indicated in each plot. End point RT-PCR of the entire RPS12 editing domain was performed using PerfeCTa SYBR Green FastMix (Quanta) with specific primers the targeting 5′ and 3′ UTR sequence and analyzed on 8% native acrylamide gels as in our previous studies (11). All amplicons in this and our previous studies were verified by cloning and manual sequencing. cDNA at different dilutions and no-RT controls were tested to confirm the linearity and specificity of the amplifications. Quantitative densitometry was done using Quantity One 1-D analysis software. Measurements were adjusted after subtraction of a background value determined from a blank lane in each blot.

Homology Modeling and Bioinformatic Analysis—Domain annotations in REH2, including the dsRBD, DEXDc, HELICc, HA2, and the previously unidentified OB fold domain were performed using the Conserved Domain Search tool (CD-Search) at the NCBI (36). A homology model of the helicase portion (residues 1308–1846) of *T. brucei* REH2 was generated using the program Phyre2 (37). The model was refined with KoBaMIN (38). The coordinates of the ADP were from the crystal structure of a yeast Prp43p-ADP complex (PDB code 2XAU) (39) after superposition of the crystal structure of this complex onto the homology model of REH2. The high quality of the geometry around the ADP binding site suggests that this part of the homology model was reliable. Sequence analysis of the gene for ^{H2}F1 suggested the presence of eight zinc finger domains of the C2H2 type. An initial homology model of ^{H2}F1 made with I-Tasser (38) failed to give all of the α helices expected in the predicted zinc fingers. Cys CB-His CG distance restraints were applied in a second run of I-Tasser. The homology model that was returned had geometry that led to the automated identification of three zinc fingers with the zincs placed (gray balls by Zfn5, Znf7, and Znf8). In addition, a DNA ligand was automatically proposed by I-Tasser because of the similarity of the position of some of the zinc finger domains in the homology model, with the crystal structure of a designed six-zinc finger DNA binding domain bound to DNA (PDB code 2I13, Ref. 40). The multiple alignment sequence analysis of the ^{H2}F1 zinc finger domains was done with BOXSHADE version 3.21.

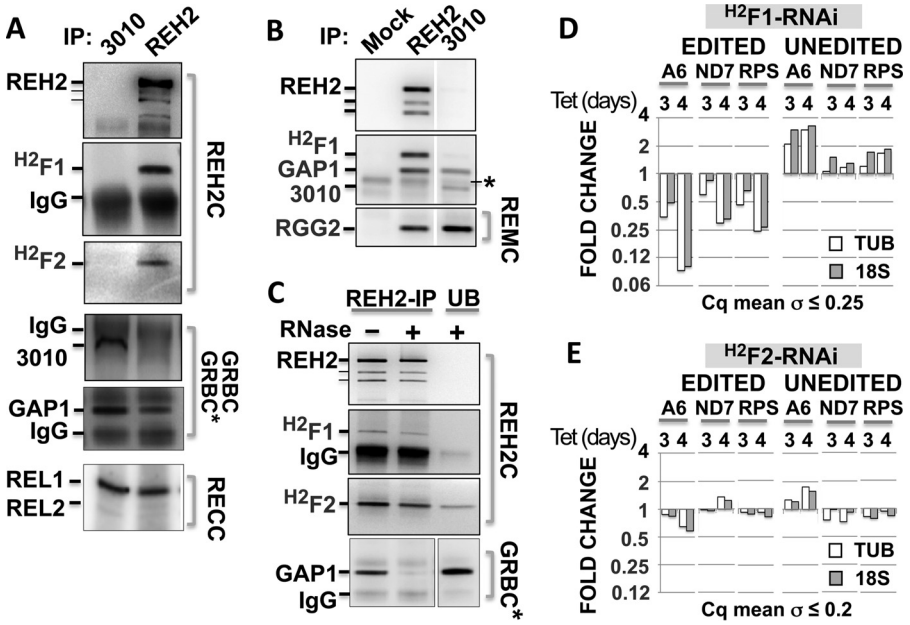

FIGURE 2. **The REH2 cofactors ^{H2}F1 and ^{H2}F2.** *A* and *B*, Western blotting of REH2-IPs and 3010-IPs. Shown are components of REH2C, GRBC*, GRBC, RECC, and REMC. The editing ligases REL1 and REL2 were assayed by ^{32}P autoadenylation. REL2 was not detected in most gels because of precharging with endogenous ATP. IgG in IPs was often faint (*asterisk*). *C*, Western blotting of REH2-IP or unbound material (*UB*) ± RNase. *D* and *E*, -fold change of mRNA transcript levels in ^{H2}F1 and ^{H2}F2 knockdowns after tetracycline (*Tet*) induction. Two biologically distinct samples with similar induction conditions (days 3 and 4) were examined in parallel measurements. qRT-PCR in ΔΔCq calculations was normalized to uninduced cells (set at 1) and tubulin (*TUB*) or 18S rRNA references. The standard deviation of the average value in Cq duplicates for each measurement is shown as the maximum deviation observed in the analysis.

Recombinant Proteins—His$_6$-REH2 (residues 1261–2167) and MBP-TEVrs*-^{H2}F1 (TEVrs: TEV recognition site, full-length ^{H2}F1) were amplified by PCR. The final products were cloned in the expression vectors pET15b (for REH2) and pMALX-B (for ^{H2}F1) (41). The purified plasmids were transformed in *Escherichia coli* Rosetta2 DE3 for protein expression. Two liters of culture for each cell line was grown at 37 °C in Terrific broth. At ~0.8 A_{600}, the temperature was reduced to 22 °C, and protein overexpression was induced with 0.5 mM isopropyl 1-thio-β-D-galactopyranoside for 22 h with shaking at 100 rpm. The harvested cells for both recombinant proteins were mixed together and stored at −80 °C for 60 h. The combined cell pellets of His$_6$-REH2 and MBP-TEVrs-^{H2}F1 were resuspended in 50 mM Tris-HCl (pH 8.5), 1 M NaCl, 20 mM 2-mercaptoethanol including 10 μg of RNase-free DNase and 15 mg of hen egg white lysozyme. Cells were lysed in an Emulsiflex hydraulic press. Cell debris was removed at 18,000 rpm for 30 min at 4 °C. The supernatant with His$_6$-REH2 and MBP-TEVrs*-^{H2}F1 was batch attached to equilibrated Qiagen nickel-nitrilotriacetic acid-agarose at 4 °C for 16 h. The complex was eluted with 50 mM Tris-HCl (pH 8.5), 1 M NaCl, 20 mM 2-mercaptoethanol, and 250 mM imidazole. The first elution of the purification was tested in native gels, Western blotting analyses, and antibody pulldowns for the presence of both recombinant proteins and the complex.

Results

Subunits of the Novel REH2-associated Subcomplex (REH2C)—We recently reported an ~15S REH2-associated subcomplex (REH2C) that contains a ~30 kDa RNA-binding protein and resists extensive RNase treatment (11). REH2C binds stably via RNA to the GRBC* subcomplex, which contains GAP1 and gRNA but lacks 3010 (11). We distinguish GRBC* from the GRBC variant (also termed MRB1 core) by their content of 3010 and some gRNAs (Fig. 2, *A* and *B*) (9). Native REH2C-GRBC* and GRBC are isolated via IP of REH2 and 3010, respectively (*i.e.* as part of mRNA-bound MRBs in prior work) (9, 11). These MRBs also associate with RGG2 and RECC (9, 11). RGG2 is the typifying subunit of another proposed subcomplex REMC or set of related subcomplexes containing RGG2 (10, 12, 20). Therefore, this study examines the bipartite REH2C-GRBC* and GRBC. Both stable particles bind tightly to REMC (in MRBs) and weakly to the RECC enzyme (forming editosomes) (Fig. 2, *A* and *B*).

To identify the subunits of REH2C, we performed a spectrometric analysis of a REH2 IP from RNA-depleted mitochondria in RNA polymerase knockdown cells as in our previous study (11). Removal of a C-terminal tag during affinity purification of this helicase was not efficient (15). Among a large number of proteins detected in the REH2 IP, a 28.8-kDa polypeptide (Tb927.6.2140) was prominent. This protein has not been studied but was observed in a purification of REH2 from normal mitochondrial extracts treated with RNase and of TbRGG1 without RNase (15, 42). Affinity purification of TAP-tagged Tb927.6.2140 showed REH2 and a 58-kDa polypeptide (Tb927.6.1680) with high confidence scores. The latter protein was found in prior purifications of REH2 and other MRB1 proteins (15, 18, 43). We will refer to Tb927.6.1680 and Tb927.6.2140 as REH2-associated factors 1 and 2 (^{H2}F1 and ^{H2}F2), respectively. Because of the high molecular mass of REH2 (242 kDa), we expected a small number of proteins in the ~15S REH2C. Consistent with their stable association in REH2C, we detected REH2, ^{H2}F1, and ^{H2}F2 in Western blotting

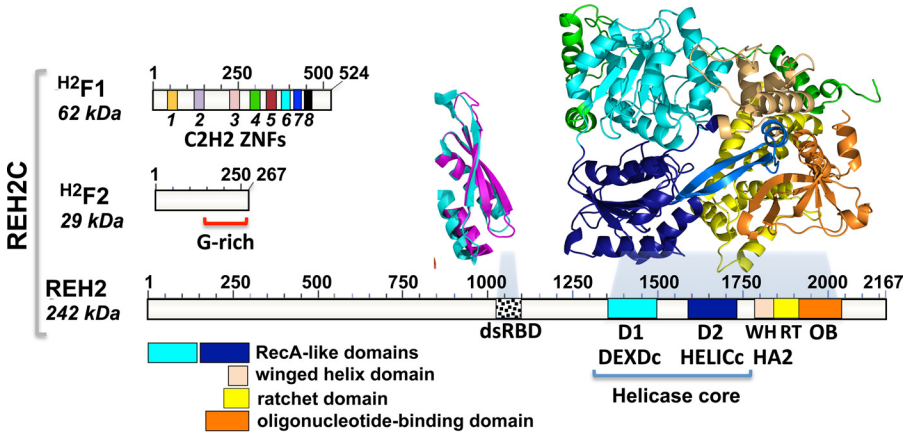

FIGURE 3. **Domain organization of REH2, ^{H2}F1, and ^{H2}F2.** Maps at scale of REH2 and its cofactors. Protein domains are color-coded in the domain map and in the structure model of REH2 (*right*) and ^{H2}F1 (*left*). REH2 conserved features in a homology model made using ADP-bound Prp43p (PDB code 2XAU) as a template. The conserved features include tandem RecA-like domains (DEXDc and HELICc in current domain databases) in the helicase core that are common to the SF1 and SF2 helicase superfamilies. After the large helicase core, there is a cluster of small domains that includes a winged helix and ratchet (annotated as helicase-associated domain HA2 in domain databases) and an OB fold. This cluster is unique to RHA-type helicases. REH2-specific sequences or elements are depicted in *green*. A few RHA-type helicases, including REH2, have a dsRBD. In our model of the REH2 dsRBD, the Tb protein is shown in *magenta*, and the structure used as a template (PDB code 1DI2) is shown in *cyan*.

analyses of REH2 IPs but not in 3010 IPs (Fig. 2*A*). Also, REH2 copurification with ^{H2}F1 and ^{H2}F2 was impervious to RNase treatment (Fig. 2*C*). Some ^{H2}F2 was found in the unbound fraction from samples with or without RNase treatment (Fig. 2*C* and data not shown). This suggests that ^{H2}F2 is not always associated with REH2 in mitochondria. Stable copurification of REH2C with GRBC* was disrupted by RNase treatment (Fig. 2*C*).

A reported, RNAi-based knockdown showed that ^{H2}F1 down-regulation inhibits editing (17). We confirmed that ^{H2}F1 knockdown induces a robust editing phenotype (Fig. 2*D*). It is common to find that accumulation of unedited pre-mRNA is not equivalent to the decrease in edited mRNA in RNAi knockdowns (11, 17). This may reflect differences in transcript stability. RNAi constructs directed to the open reading frame or the 3′ UTR of ^{H2}F2 did not seem to affect *in vivo* editing of the tested substrates (Fig. 2*E* and data not shown). Therefore, we identified two REH2 cofactors, ^{H2}F1 and ^{H2}F2. However, only ^{H2}F1 was associated with editing of the tested substrates in procyclics.

Domain organization of REH2, ^{H2}F1, and ^{H2}F2—Crystallographic studies of monomeric superfamily 1 (SF1) and SF2 helicases revealed a catalytic core with tandem RecA-like domains (annotated in domain databases as DEXDc and HELICc) and characteristic motifs (I-VI) in ATP-binding/hydrolysis, RNA binding, and unwinding (39). The first crystal structure in the DEAH/RHA family that comprises a number of nuclear and cytosolic proteins revealed a specific C-terminal cluster with winged helix, ratchet, and OB fold domains (39). The winged helix and ratchet domains are annotated as the "helicase-associated domain" HA2. Our homology model of REH2 showed this domain cluster (Fig. 3). The C-terminal OB fold in REH2 was detected in a sequence analysis (45), but the domain cluster is only recognized in the three-dimensional structure. So, this molecular design is found in a mitochondrial helicase in trypanosomes and predates the evolutionary split of trypanosomes from other eukaryotes that occurred over 100 million years ago (46). This model was generated with part of *T. brucei* REH2 (residues 1308–1846), using as a template the crystal structure of a yeast Prp43p-ADP complex (PDB code 2XAU) (39). The coordinates of the ADP were found after superposition of the crystal structure of the complex onto the homology model of REH2. The high quality of the geometry around the ADP binding site suggests that this part of the homology model is reliable.

REH2 and a few members in the RHA subfamily also contain a canonical dsRNA-binding domain (dsRBD) with an α1-β1-β2-β3-α2 fold that binds dsRNA (Fig. 3) (47). ^{H2}F1 has eight potential Cys^2His^2 zinc fingers (Znf1–8) (Fig. 3 and data not shown). A search for conserved domains (36) identified Znf5 as a dsRNA-binding domain (pfam12171; E value, 7.05e-03) originally reported in JAZ dsRNA-binding Znf proteins (48). The conserved domain database search predicted Znf6–8. Three zinc fingers (Zfn5, Znf7, and Znf8) were accurate enough in the homology model of ^{H2}F1 for the coordination of zinc atoms. Also, a DNA ligand has been proposed because of the similarity of the position of some of the zinc finger domains in the homology model with the crystal structure of a designed six-zinc finger DNA binding domain bound to DNA (PDB code 2i13) (40) (data not shown). Although we were able to fit a DNA double helix on the basis of available domain databases, we expect specific ^{H2}F1 binding to helical RNA structures in the context of trypanosome editing. We identified Znf1–4 after visual inspection and a sequence alignment of all fingers in ^{H2}F1 (data not shown). ^{H2}F2 has a conserved hydrolase domain (cl11421) (15) spanning most of its length. Also, the C-terminal half of this small polypeptide is rich in glycine. This feature of ^{H2}F2 is reminiscent of G-patch proteins, including several helicase partners in the RHA family (49). G-patch proteins carry one or more copies of a glycine-rich domain (G-patch domain) defined by seven conserved glycines. This motif is not obvious in ^{H2}F2, but this protein may be a diverged member in the family of G-patch proteins.

REH2C and mRNA Form a Stable mRNP in the Absence of GAP1 and gRNA—We hypothesized that REH2C binds mRNA directly. This idea is consistent with the findings that REH2

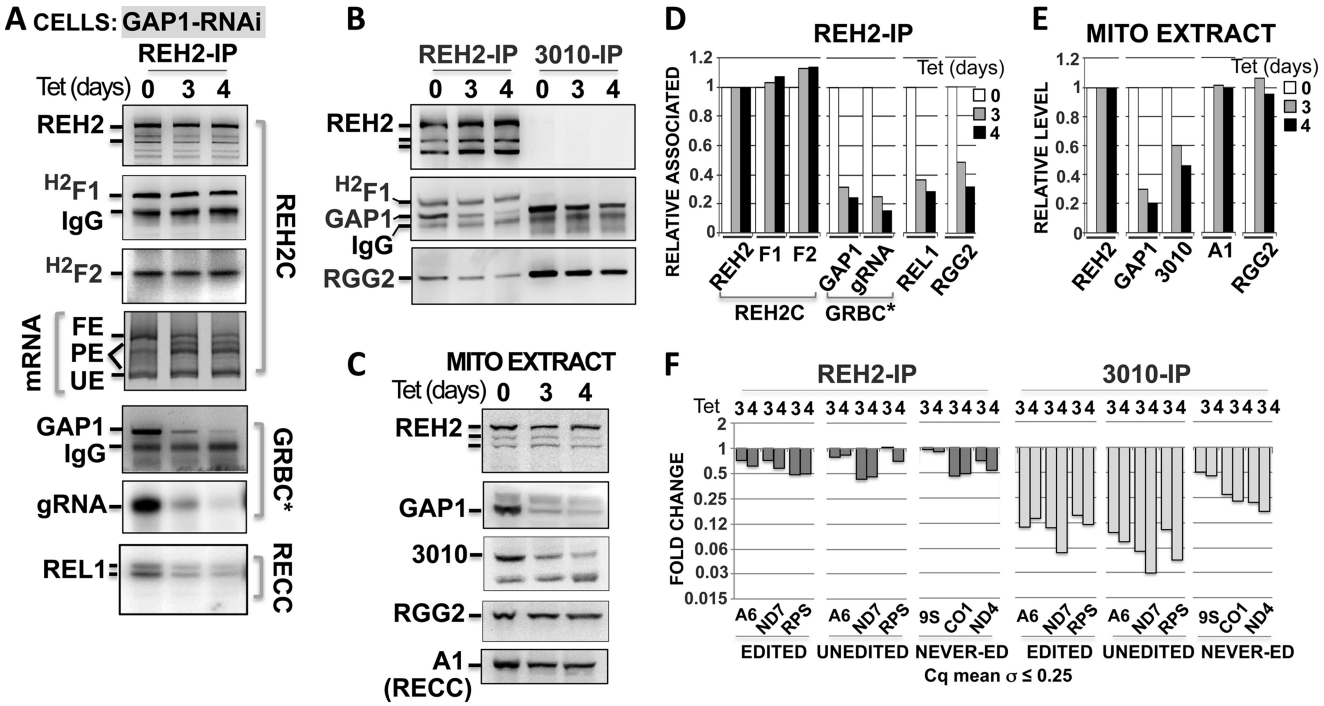

FIGURE 4. **REH2C is an mRNP.** *A–C*, analyses as in Fig. 2*A* of REH2-IPs and 3010-IPs from GAP1-RNAi extract (*A* and B) and total mitochondrial (*MITO*) extract (*C*). KREPA1 (*A1*) is a core subunit of RECC. In *A*, total gRNA and mRNA RPS12 (*FE*, fully edited; *PE*, partially edited; *UE*, unedited) were assayed by ^{32}P capping and RT-PCR, respectively. Our cell line had two REL1 isoforms that were clearly resolved in some gels. *D*, densitometry of the proteins and gRNA in *A*. RGG2 was scored from *B*. Relative association was double-normalized to recovered REH2 in IPs and each component at day 0 (set at 1). *E*, densitometry of the proteins in *C*. Values were double-normalized to recovered REH2 and to day 0. *F*, -fold change in the levels of bound edited and unedited mRNAs in IPs in GAP1 RNAi cells. The ratio of mRNA in the IPs and total mtRNA input on days 3 and 4 of induction was compared with the same ratio in uninduced samples (day 0 set at 1). qRT-PCR calculations were normalized to a mock IP and input values. Standard deviation of the average value in Cq duplicates is the maximum deviation observed in the duplicates.

binds RNA, inactivating point mutations in REH2 hinder mRNA association with native REH2C-GRBC* (in *cis*), and depletion of REH2 reduces pre-mRNA association with GRBC (in *trans*) (11, 15). Because GAP1 binds and stabilizes gRNA (18), we surmised that an mRNP with REH2C and mRNA could be isolated from GAP1-depleted mitochondria. As expected, RNAi-based GAP1 knockdown removed most GAP1 and gRNA (GRBC*) in the REH2 pulldowns. However, loss of GRBC* did not affect the integrity of REH2C (Fig. 4, *A–E*, and data not shown) or the steady-state level of RECC and REMC core proteins in the parasites (Fig. 4, *C* and *E*, and data not shown). These data indicate that the protein integrity of REH2C is independent of gRNA-associated subcomplexes.

REH2C retained a substantial association with pre-mRNAs substrates, editing intermediates, and fully edited transcripts in the GAP1 knockdown. Two complementary analyses applied in a previous study of isolated complexes have shown this (11). First, end point RT-PCR gels of mRNA RPS12, using primers directed to a never-edited UTR sequence, showed a similar level of unedited pre-mRNA in all REH2 pulldowns (Fig. 4*A*). GAP1 knockdown caused a robust editing phenotype with gradual accumulation of partially edited RNA species and a concurrent decrease of fully edited mRNA when comparing 0, 3 and 4 days of induction. Second, qRT-PCR of unedited and fully edited transcripts in IPs, normalized to both a mock pulldown and input (loaded extract) values, showed REH2C retention (~50% or higher) of the tested transcripts in mitochondria depleted of GAP1 and gRNA (Fig. 4*F*). This indicates that the REH2C subcomplex is a stable mRNP particle.

In contrast, at least ~90% of unedited pre-mRNA and edited transcripts were lost in 3010 IPs from GAP1-depleted extracts Fig. 4*F*). This was explained in part by a ~60% decrease in total 3010 in these extracts (Fig. 4, *C* and *E*). Despite a moderate reduction in 3010, the greater depletion of cellular GAP1 and gRNA (~80%; Fig. 4, *C* and *E*, and data not shown) matched more closely the dramatic loss of mRNA in 3010-IPs. This suggested that mRNA retention by GRBC requires gRNA. In practice, two time points of RNAi induction (days 3 and 4) in the analyses provided biological replicates of the effects relative to uninduced cells. As noted above, the cellular level of RECC and REMC proteins was normal in the GAP1 knockdown. However, the amount of these complexes decreased in REH2 pulldowns from these cells (Fig. 4, *A*, *B*, and *D*). Therefore, normal association of REH2C with RECC enzyme and REMC requires GRBC* (or another subcomplex in the MRBs).

The normal steady-state level of RGG2 in cells depleted of either GAP1 (Fig. 4, *C* and *E*) (10) or REH2 (11) is consistent with the idea that REMC (typified by RGG2) is a separate subcomplex in the editing scaffolds. The presence of 9S rRNA and never-edited mRNA transcripts in IPs of REH2 and 3010 reflects a transient association of mitoribosomes with native editing complexes (9, 11). These transcripts showed a moderate decrease in IPs from GAP1-depleted extracts. This suggested an interaction of REH2C with at least some mitoribosomes in

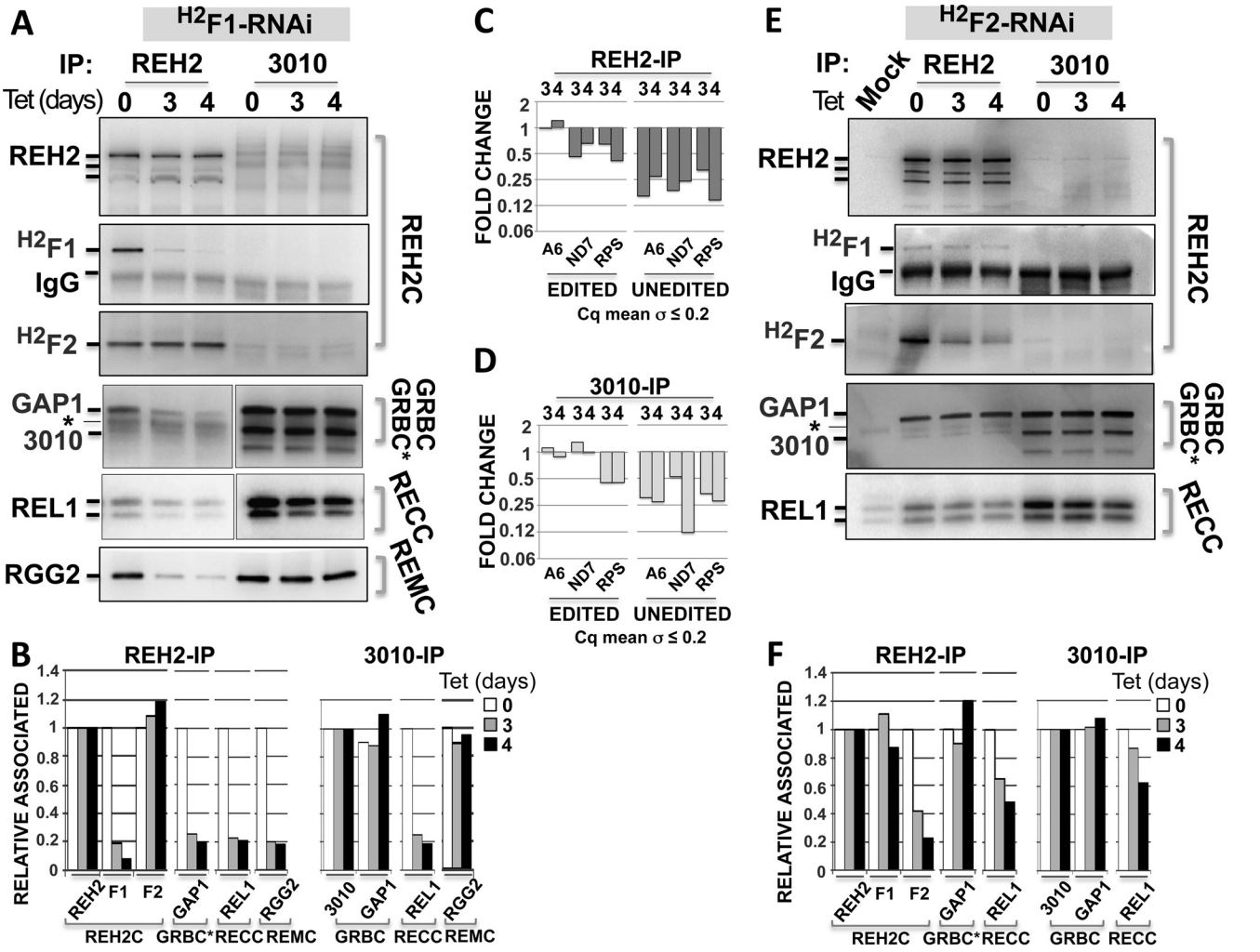

FIGURE 5. **Effects of ^{H2}F1 or ^{H2}F2 knockdown on the association between REH2C, GRBC*, GRBC, REMC, and RECC.** *A* and *E*, analysis as above of protein components in IPs from RNAi extracts. A mock IP was included in *E*. The IgG band in IPs was often faint (*asterisk*). *B* and *F*, densitometry of *A* and *E*, respectively. *C* and *D*, -fold change in the levels of bound edited and unedited mRNAs. The ratio of mRNA in the IPs and total mtRNA on days 3 and 4 of induction was compared with the same ratio in uninduced samples (day 0 set at 1). Standard deviation of the average value in Cq duplicates is the maximum deviation observed in the duplicates.

the absence of GRBC* (Fig. 4*F*). It is possible that the remaining 3010-associated particles in these cells also retain some mitoribosomes. We observed an accumulation of mitoribosomes in 3010-IPs that requires REH2 (11). Note that our plots indicate the relative change in transcript abundance in the IPs (not total content). Induced samples were normalized to uninduced samples (see figure legends and "Experimental Procedures"). Never-edited mRNAs occur at a low level in 3010-IPs and REH2-IPs. Edited and unedited mRNAs are relatively enriched in the same samples (9). The above data showed that the REH2C subcomplex includes all mRNA types in editing, and that the integrity of this mRNP does not need GRBC* in *cis* or GRBC in *trans*. The data also imply that the assembly of substrate-loaded editing scaffolds involves coupling of specialized RNPs (an mRNP (REH2C) and gRNP variants (GRBC or GRBC*)) via specific base pairing between their mRNA and gRNA cargo, respectively.

Cis and Trans Effects of ^{H2}F1 on Native REH2- and 3010-purified Editosomes, Assembly of RNP Modules, Pre-mRNA Loading, and Transient Interaction with RECC—We examined ^{H2}F1 for possible *cis* and *trans* effects on the assembly of editing scaffolds with mRNA and transient interaction with RECC enzyme. The depletion of ^{H2}F1 did not prevent formation of an ^{H2}F2-REH2 subcomplex but eliminated nearly 80% of its association with GRBC*, REMC, RECC, and pre-mRNA (in REH2-IPs; Fig. 5, *A*–*C*). Therefore, ^{H2}F1 has strong *cis* effects on protein-RNA interactions in REH2-bound complexes. In *trans*, ^{H2}F1 depletion did not compromise the integrity of the GRBC subcomplex but clearly reduced its association with RECC and pre-mRNA (in 3010-IPs; Fig. 5, *A*, *B*, and *D*). All proteins tested had a normal steady-state level in ^{H2}F1-depleted cells. We confirmed this in replica IPs and in total mitochondrial extract, including a core subunit of RECC (data not shown). Also, pre-mRNAs in these cells were stable or accumulated slightly (Fig. 2*D*) (18). Therefore, a clear loss of RECC in both REH2-IPs and 3010-IPs from ^{H2}F1-depleted mitochondria suggested that ^{H2}F1 promotes the addition of the RECC enzyme to editing scaffolds both in *cis* and in *trans*. In line with our GAP1-depletion experiments shown in Fig. 4, loss of GRBC* and REMC in REH2-IPs, but normal retention of GRBC and REMC in 3010-IPs from the ^{H2}F1 knockdowns, show that the GRBC*-REMC and GRBC-REMC aggregates are tightly bound in scaffolds

purified via REH2 or 3010, respectively. We note that the stability of REH2, but not ^{H2}F2, appeared to be slightly compromised after ^{H2}F1 depletion both in REH2-IPs and mitochondrial extract (Fig. 5*A* and data not shown). Still, the decrease in REH2 full-length is severalfold less than the large loss of GAP1 and RECC in REH2 IPs (Fig. 5*A* and data not shown). Therefore, loss of ^{H2}F1 induced clear effects on editosome assembly and pre-mRNA association. In these experiments, we plotted the level of proteins normalized to REH2 full-length in the pulldowns (Fig. 5, *B* and *F*). As in Fig. 4, two time points of RNAi induction (on days 3 and 4) enable the analysis of biologically distinct samples under similar conditions.

We note that the steady-state level of the tested subunits in GRBC, REMC, and RECC appeared normal in the ^{H2}F1 knockdown. This was clear in 3010-purified GRBC and in mitochondrial extracts from ^{H2}F1-depleted cells (Fig. 5*A* and data not shown). This indicated that the cells were viable at the examined time points of RNAi induction. Down-regulation of ^{H2}F2 did not prevent formation of a ^{H2}F1-REH2 subcomplex and had no evident effects on REH2 stability or the assembly of ^{H2}F1-REH2 with GRBC*. Also, the integrity of GRBC was normal. A slight decrease in RECC was detected in both IPs of REH2 and 3010 (Fig. 5, *E* and *F*), but no evident editing phenotype was found in the tested substrates, as shown above. The steady-state level of RECC, examined in Western blotting analyses of a core subunit, was normal in the ^{H2}F2 knockdown (data not shown). Therefore, ^{H2}F2 may affect the formation of higher-order complexes in mitochondria that include the RECC enzyme but is not essential for editing.

In summary, these data show that ^{H2}F1 affects the coupling of REH2C with GRBC* (in *cis*) and the association of RECC and pre-mRNA with the editing scaffolds (in *cis* and in *trans*). This agrees with a model in which stable or transient docking of mRNP and gRNP modules involves the specific base pairing of their mRNA and gRNA cargo.

Depletion of REH2 Helicase Dissociates ^{H2}F1 from ^{H2}F2 but Moderately Affects the ^{H2}F1 Association with Other Editosome Components—We asked whether ^{H2}F1 associates with components of native REH2-purified editosomes in REH2-depleted mitochondria. ^{H2}F1 IPs from REH2 knockdown cells exhibited a comparable loss of REH2 and ^{H2}F2. This is consistent with the idea that REH2 associates directly with ^{H2}F2 (Fig. 6, *A* and *B*). Despite a large loss of REH2 and ^{H2}F2 in the ^{H2}F1 IPs from REH2 knockdown cells, there was a moderate decrease in ^{H2}F1 association with GRBC*, REMC, and RECC. This suggested that ^{H2}F1 supports some interaction with GRBC* and RECC in these cells. It also implied added complexity in the network of interactions that control the assembly of editosomes.

Native REH2 purifications exhibit a 3′-5′ unwinding activity of short RNA duplexes that requires ATP as well as dsRBD and ATPase domains of REH2 (15). This REH2-dependent unwinding activity was observed in ^{H2}F1 pulldowns from normal but not REH2-depleted extracts (Fig. 6*C*). This is in line with the idea that REH2 is the major source of the RNA unwinding activity in our assays using short dsRNA and immunopurified native editing complexes.

Therefore, ^{H2}F1 may keep some interactions with components of native editosomes under conditions of REH2 down-

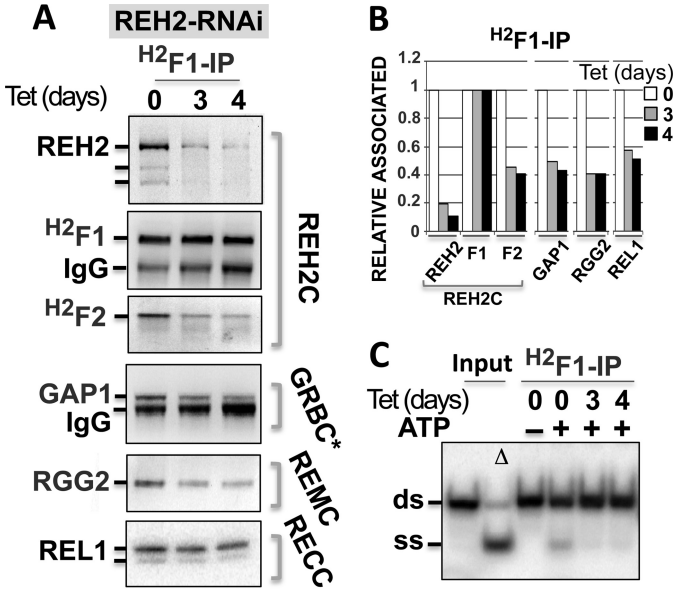

FIGURE 6. **Effects of REH2 knockdown on the ^{H2}F1 association with ^{H2}F2, GRBC*, REMC, and RECC.** *A*, analyses as above of protein components in ^{H2}F1-IPs from REH2-RNAi extracts. *B*, densitometry of *A*. *C*, unwinding assays with a radiolabeled RNA duplex substrate in mixtures ± exogenously added 2 mM ATP.

regulation. However, REH2 is necessary for optimal ^{H2}F1 stable association with GRBC* and transient contact with the RECC enzyme.

^{H2}F1 Promotes, in cis and in trans, the Formation of Stable RNPs with a Short RNA Duplex—As expected, we detected the unwinding of the short dsRNA described above in REH2 IPs but not in 3010 or mock IPs (Fig. 7*A*). Interestingly, this dsRNA substrate in the unwinding assays also formed gel retardation products in REH2 IPs and 3010 IPs. These products indicated a stable association of the short dsRNA with the immunopurified native complexes. These RNPs were sensitive to proteinase K (data not shown) and co-migrated with RECC enzyme in identical IPs (Fig. 7*B*). ^{H2}F1 depletion reduced the accumulation of RNPs containing REH2 or 3010 in *cis* and in *trans*, respectively, but had little or no effect on the unwinding activity of the REH2-purified complex (Fig. 7*C*). GAP1 knockdown also decreased formation of the purified RNPs (Fig. 7*D*). Therefore, the RNPs detected with a short radiolabeled RNA duplex represent RNA-bound editosomes. In line with our model of editosome assembly, REH2 and ^{H2}F1 in the mRNP and GAP1 in the gRNP variants are required for docking of RNPs in higher-order editing complexes.

Recombinant REH2 and ^{H2}F1 Proteins Associate with Each Other in a Complex in Vitro—We expressed His_6-REH2 (residues 1261–2167, ~100 kDa) and MBP-TEVrs*-^{H2}F1 (~100 kDa) in bacteria. To determine whether these two recombinant proteins form a complex *in vitro*, we mixed bacterial extracts of each protein and purified His_6-REH2 from the mixture by affinity chromatography. In native gels, the eluted sample contained two or three main species that could represent free His_6-REH2 and complexes between His_6-REH2 and MBP-TEVrs*-^{H2}F1 (Fig. 8*A*). We confirmed that both His_6-REH2 and MBP-TEVrs*-^{H2}F1 were present in the eluted sample (Fig. 8, *B* and *C*). IPs of ^{H2}F1 contained His_6-REH2, and IPs of REH2 contained

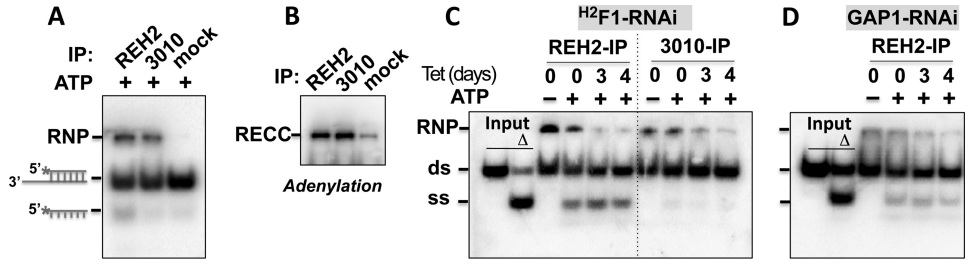

FIGURE 7. **Analysis of REH2 and 3010 purified complexes for unwinding activity and formation of an RNP with a short radioactive RNA duplex.** *A*, assays of unwinding activity and RNP formation in REH2, 3010, and mock IPs with 2 mM ATP. *B*, radioactive autoadenylation of editing ligases in complexes that co-migrate with the RNPs in *A*. *C* and *D*, assays as in *A* but from ^{H2}F1-RNAi or GAP1-RNAi extracts on days 0, 3, and 4 of induction ± ATP.

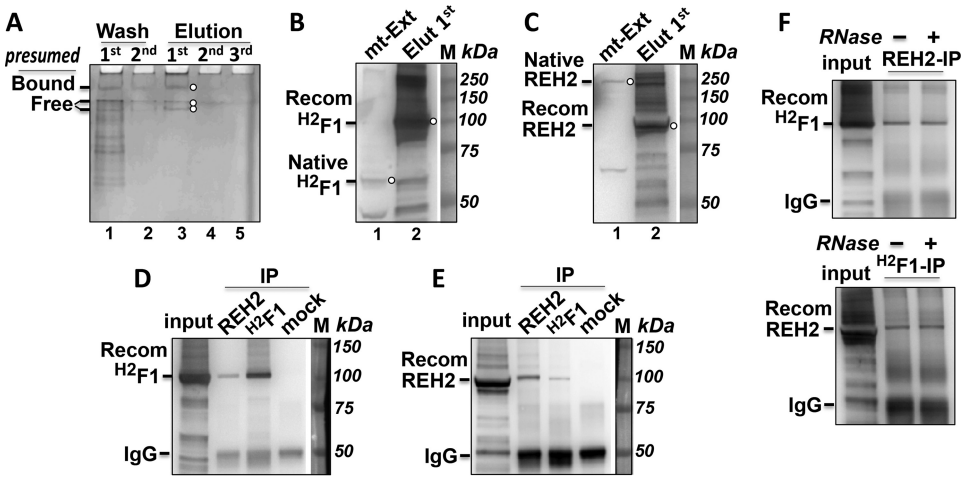

FIGURE 8. **Recombinant REH2 and ^{H2}F1 proteins copurified in a complex.** *A*, silver-stained native gel of a purification of His_6-REH2 from an extract mixture that also contained MBP-TEVrs*-^{H2}F1: washes (*lanes 1–2*) and elutions (*lanes 3–5*). Presumed bound proteins in a complex or free are indicated. *B* and *C*, SDS-PAGE Western blot analyses of mitochondrial extract (*mt-Ext*, *lane 1*) or first elution (*Elut 1st*) from *A* (*lane 3*). *M*, marker lane. *D* and *E*, SDS-PAGE Western blotting analyses of the first elution from *A* (*input*) or IPs of this fraction with anti-^{H2}F1, anti-REH2, or irrelevant antibodies (*mock*). *F*, RNase A/T1 treatment of the recombinant ^{H2}F1-REH2 complex while bound to the beads in REH2 or ^{H2}F1 IPs.

MBP-TEVrs*-^{H2}F1 (Fig. 8, *D* and *E*). Finally, in IPs of REH2 or ^{H2}F1, the complex resisted RNase digestion (Fig. 8*F*). Therefore, these recombinant versions of REH2 and ^{H2}F1 form a stable complex. Direct association between these proteins in the REH2C subcomplex is consistent with the slight destabilization of REH2 we observed in ^{H2}F1-depleted cells (Fig. 5*A* and data not shown).

Discussion

These results support the hypothesis that the REH2C subcomplex controls the assembly and function of editosomes. A long standing question is how RECC may reach editing substrates *in vivo*. Because MRB1 complexes contain pre-mRNA substrates and products of editing, we and others proposed that these complexes serve as scaffolds for specific assembly of mRNA-gRNA hybrid substrates and their processing by RECC (9, 10). This study adds several new insights to our model of assembly and regulation in higher-order editosomes. This model is on the basis of a new conceptual framework in which MRB1 complexes include physically and functionally distinct RNPs (Fig. 9): the catalytic mRNP REH2C with mRNA, the helicase REH2, and specific cofactors and structural gRNP variants (GRBC and GRBC*) with multiple gRNAs and several proteins of MRB1 (data now shown) (9). GRBC, including 3010, is also called MRB1 core (12).

REH2C Is an mRNP with Pre-RNA Substrates, Intermediates, and Products of Editing—We proposed docking of mRNP and gRNP modules through specific base pairing of their respective mRNA and gRNA cargo, respectively. This model is consistent with our finding that REH2C retains mRNA editing substrates and products at nearly normal levels upon depletion of GAP1 and gRNA in mitochondria. Therefore, the REH2C mRNP can be physically uncoupled from GRBC variants that carry and stabilize gRNA. Docking of the helicase mRNP with GRBC* is stable. In contrast, the interaction between mRNP and GRBC involves transient contacts. Either type of RNP association may stabilize hybrid substrates on the scaffolds that engage the RECC enzyme. Therefore, in the mitochondrial milieu, a target search by small gRNAs is likely a protein-assisted process (Fig. 9). This model is also consistent with our prior identification of *cis* and *trans* effects of REH2 (11). Inactivating mutations in the helicase core or dsRBD motifs uncouple REH2 from GRBC* and mRNA substrates and products and RNAi-based depletion of REH2 reduce pre-mRNA content and editing progression of mRNAs bound to GRBC. Similar target search mechanisms by base pairing of guide RNA with target RNA or DNA occur in RNA silencing, mRNA splicing, and rRNA biogenesis in eukaryotes and gene expression control by small regulatory RNAs and clustered regulatory interspaced short palindromic repeats RNAs in prokaryotes (50).

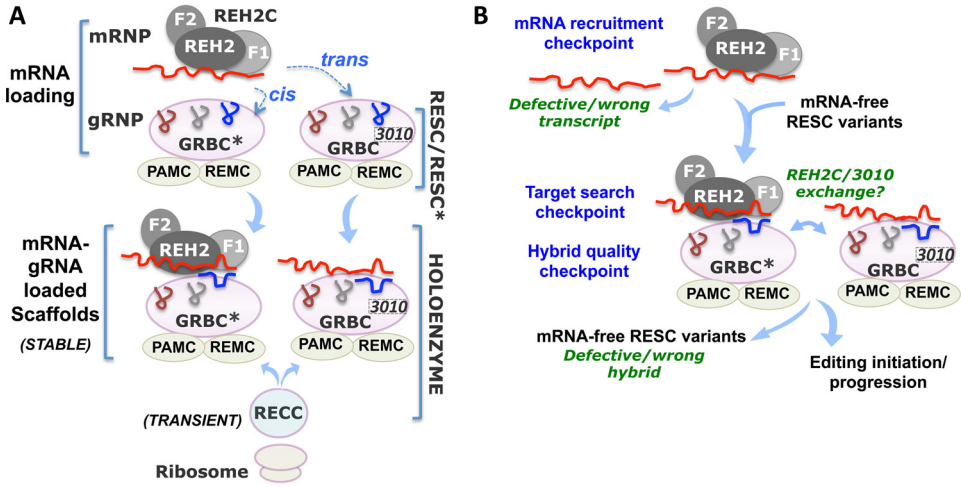

FIGURE 9. **Model of mRNP and gRNP docking and specificity checkpoints in editosomes.** *A*, assembly of mRNA-gRNA hybrid substrates on accessory editing scaffolds involves docking of mRNP and gRNP modules that hold mRNA and gRNA, respectively. In the proposed model, RNPs are joined via specific base pairing of mRNA and gRNA. The REH2 and ^{H2}F1 subunits in the mRNP (termed REH2C) control mRNA substrate loading in *cis* or *trans* onto the gRNP variants GRBC and GRBC* (with and without 3010, respectively). The GRBC variants bind tightly to REMC and the polyadenylation mediator complex (*PAMC*) in tripartite aggregates labeled *RESC* and *RESC**. The REH2C-RESC interaction is transient, but the REH2C-RESC* association is stable. Transient addition of RECC to mRNA-gRNA-loaded scaffolds form editing holoenzymes or editosomes. Mitoribosomes are also added in post-editing interactions. *B*, critical checkpoints in the editing pathway are expected during mRNA recruitment, target search, and scrutiny of hybrid quality in substrate-bound scaffolds. The regulatory C terminus of REH2 and multiple zinc fingers of ^{H2}F1 may function in synergy at these checkpoints. REH2 helicase activity may remodel RNA-protein assemblies and resolve secondary structure during editing. Cycles of REH2C and 3010 exchange may create REH2C-RESC* and RESC complexes.

Novel Domain Organization and Participation of REH2 and ^{H2}F1 in RNA Editing—REH2 is the first identified RHA-type protein that participates in a eukaryotic RNA editing system. The conserved CTD of REH2 is an ancient molecular design that predates the origin of trypanosomes over 100 million years ago (46). It offers a unique opportunity to probe conserved features that may affect helicase function in REH2 and related eukaryotic proteins in transcription, mRNA splicing, silencing, and innate immunity (39, 44). Specific CTD determinants may control different steps of the editing pathway, such as mRNA recruitment by REH2C, docking of mRNP and gRNP modules, and addition of RECC or editing progression in the molecular scaffolds. The OB fold in other RHA-type helicases interacts with helicase cofactors and RNA that often modulate ATPase and unwinding activities of the helicase (49). The CTD may control the REH2 binding with ^{H2}F1 we found with recombinant proteins (Fig. 8). The unique ~1000-residue-long N-terminal region lacks identifiable domains. The N-terminal region could provide additional editing determinants or a docking surface for factors in other mitochondrial RNA processes, including mitoribosomes. In a prior study, we proposed that REH2-purified complexes could serve as "organizers" in mitochondrial RNA metabolism (15). Ongoing work in our laboratory is characterizing the conserved CTD and the unique N-terminal region in REH2. ^{H2}F1 is related to a specialized class of Cys^{2}His^2 zinc finger (Znf) proteins that usually bind to dsRNAs. Several dsRNA-binding Znf proteins (dsRBZFPs) play important roles in cellular localization and apoptosis (48). These proteins have several domains, each containing zinc finger motifs, and each is capable of binding dsRNA. The mammalian JAZ protein has four Znf domains (51), the zinc finger protein ZFa has seven (52), and ^{H2}F1 potentially has eight (data not shown). Although all Znf domains in ^{H2}F1 may contribute to dsRNA binding, some Znf domains could also mediate direct protein interactions with REH2. This is currently being addressed in our laboratory.

Requirements for Assembly of Native Higher-order Editosomes—Genetic knockdown of ^{H2}F1 had differential *cis* and *trans* effects on native editosomes (Fig. 5). For example, ^{H2}F1 depletion did not affect the formation of a ^{H2}F2-REH2 subcomplex but decreased its association with mRNA (particularly pre-mRNA), GRBC*, REMC, and RECC (in *cis*). In contrast, the GRBC-REMC complex was normal in the ^{H2}F1 knockdown, but it exhibited a decreased association with pre-mRNA and RECC (in *trans*). This result suggests that the RECC enzyme enters the pathway through interactions with preassembled mRNA-gRNA hybrids in the scaffolds rather than via mRNA in the mRNP or via gRNA in gRNPs before the RNPs interact. This model of RECC entry also agrees with the loss of copurification between REH2C and the RECC enzyme in a GAP1 knockdown. That is, in gRNA-depleted mitochondria, REH2C retained mRNA substrates and products but lost its interaction with the RECC enzyme (Fig. 4). The requirement of ^{H2}F1 for normal editing and assembly of higher-order editosomes validated ^{H2}F1 as a *bona fide* regulatory cofactor of REH2. In summary, we propose that ^{H2}F1 controls the docking between mRNP and gRNP modules. The coupling of these RNPs seems to be an essential step in the assembly of fully competent editosomes. ^{H2}F1 may promote specific pre-mRNA recruitment by REH2C. The complete mRNP then joins gRNPs via specific base pairing (Fig. 9), resulting in the assembly of stable of mRNA-gRNA hybrids. Finally, RECC is added directly to the substrate hybrids in the scaffolds. Our analysis of RGG2 in REMC is consistent with direct association of this subcomplex with GRBC and GRBC*. This implies that mitochondria contain at least two versions of the proposed tripartite GRBC/REMC/PAMC complex, also termed RESC (10).

In summary, our recent report (11) and this study indicate that REH2 and ^{H2}F1 subunits of REH2C are required to establish stable mRNA-gRNA hybrid substrates in molecular scaffolds for editing. In the proposed model of stepwise editosome assembly, specificity checkpoints may exist during initial mRNA recruitment by REH2C, subsequent target search and coupling of mRNP and gRNP via specific base pairing, and quality control of preassembled mRNA-gRNA hybrids for RECC binding and catalysis. REH2 and ^{H2}F1 may act in synchrony, likely via the regulatory C-terminal and multiple zinc finger domains, respectively, during these specificity checkpoints (Fig. 9).

Author Contributions—V. K., B. R. M., and B. P. conducted the molecular genetic and biochemical experiments. S. G., C. K., and A. S. subcloned, expressed, and purified recombinant proteins and their complexes. B. H. M. M. performed the homology modeling. A. A. V. and J. A. W. conducted the mass spectrometric analyses. L. K. R. contributed unpublished antibodies against ^{H2}F2. All coauthors critically analyzed the results. J. C. R. and the members of his laboratory conceived the idea for the project and prepared the data figures. J. C. R. wrote most of the paper with B. H. M. M. and V. K.

Acknowledgments—We thank Craig Kaplan for providing access to equipment for real-time PCR and Ken Stuart for monoclonal antibodies against core subunits of the RECC enzyme.

References

1. Cruz-Reyes, J., and Read, L. K. (2013) in *RNA Editing: Current Research and Future Trends* (Maas, S., ed.) pp 65–90, Caister Academic Press, Norfolk, UK
2. Read, L. K., Lukeš, J., and Hashimi, H. (2016) Trypanosome RNA editing: the complexity of getting U in and taking U out. *Wiley Interdiscip. Rev. RNA* **7,** 33–51
3. Aphasizheva, I., and Aphasizhev, R. (2016) U-insertion/deletion mRNA-editing holoenzyme: definition in sight. *Trends Parasitol.* **32,** 144–156
4. Rusché, L. N., Cruz-Reyes, J., Piller, K. J., and Sollner-Webb, B. (1997) Purification of a functional enzymatic editing complex from *Trypanosoma brucei* mitochondria. *EMBO J.* **16,** 4069–4081
5. Li, F., Ge, P., Hui, W. H., Atanasov, I., Rogers, K., Guo, Q., Osato, D., Falick, A. M., Zhou, Z. H., and Simpson, L. (2009) Structure of the core editing complex (L-complex) involved in uridine insertion/deletion RNA editing in trypanosomatid mitochondria. *Proc. Natl. Acad. Sci. U.S.A.* **106,** 12306–12310
6. Golas, M. M., Böhm, C., Sander, B., Effenberger, K., Brecht, M., Stark, H., and Göringer, H. U. (2009) Snapshots of the RNA editing machine in trypanosomes captured at different assembly stages *in vivo*. *EMBO J.* **28,** 766–778
7. Hashimi, H., Zimmer, S. L., Ammerman, M. L., Read, L. K., and Lukeš, J. (2013) Dual core processing: MRB1 is an emerging kinetoplast RNA editing complex. *Trends Parasitol.* **29,** 91–99
8. Aphasizhev, R., and Aphasizheva, I. (2014) Mitochondrial RNA editing in trypanosomes: small RNAs in control. *Biochimie* **100,** 125–131
9. Madina, B. R., Kumar, V., Metz, R., Mooers, B. H., Bundschuh, R., and Cruz-Reyes, J. (2014) Native mitochondrial RNA-binding complexes in kinetoplastid RNA editing differ in guide RNA composition. *RNA* **20,** 1142–1152
10. Aphasizheva, I., Zhang, L., Wang, X., Kaake, R. M., Huang, L., Monti, S., and Aphasizhev, R. (2014) RNA binding and core complexes constitute the U-insertion/deletion editosome. *Mol. Cell. Biol.* **34,** 4329–4342
11. Madina, B. R., Kumar, V., Mooers, B. H., and Cruz-Reyes, J. (2015) Native variants of the MRB1 complex exhibit specialized functions in kinetoplastid RNA editing. *PloS ONE* **10,** e0123441
12. Ammerman, M. L., Downey, K. M., Hashimi, H., Fisk, J. C., Tomasello, D. L., Faktorová, D., Kafková, L., King, T., Lukes, J., and Read, L. K. (2012) Architecture of the trypanosome RNA editing accessory complex, MRB1. *Nucleic Acids Res.* **40,** 5637–5650
13. Ammerman, M. L., Presnyak, V., Fisk, J. C., Foda, B. M., and Read, L. K. (2010) TbRGG2 facilitates kinetoplastid RNA editing initiation and progression past intrinsic pause sites. *RNA* **16,** 2239–2251
14. Aphasizheva, I., Maslov, D., Wang, X., Huang, L., and Aphasizhev, R. (2011) Pentatricopeptide repeat proteins stimulate mRNA adenylation/uridylation to activate mitochondrial translation in trypanosomes. *Mol. Cell* **42,** 106–117
15. Hernandez, A., Madina, B. R., Ro, K., Wohlschlegel, J. A., Willard, B., Kinter, M. T., and Cruz-Reyes, J. (2010) REH2 RNA helicase in kinetoplastid mitochondria: ribonucleoprotein complexes and essential motifs for unwinding and guide RNA (gRNA) binding. *J. Biol. Chem.* **285,** 1220–1228
16. Wirtz, E., Leal, S., Ochatt, C., and Cross, G. A. (1999) A tightly regulated inducible expression system for conditional gene knock-outs and dominant-negative genetics in *Trypanosoma brucei*. *Mol. Biochem. Parasitol.* **99,** 89–101
17. Acestor, N., Panigrahi, A. K., Carnes, J., Zíková, A., and Stuart, K. D. (2009) The MRB1 complex functions in kinetoplastid RNA processing. *RNA* **15,** 277–286
18. Weng, J., Aphasizheva, I., Etheridge, R. D., Huang, L., Wang, X., Falick, A. M., and Aphasizhev, R. (2008) Guide RNA-binding complex from mitochondria of trypanosomatids. *Mol. Cell* **32,** 198–209
19. Wickstead, B., Ersfeld, K., and Gull, K. (2002) Targeting of a tetracycline-inducible expression system to the transcriptionally silent minichromosomes of *Trypanosoma brucei*. *Mol. Biochem. Parasitol.* **125,** 211–216
20. Madina, B. R., Kuppan, G., Vashisht, A. A., Liang, Y. H., Downey, K. M., Wohlschlegel, J. A., Ji, X., Sze, S. H., Sacchettini, J. C., Read, L. K., and Cruz-Reyes, J. (2011) Guide RNA biogenesis involves a novel RNase III family endoribonuclease in *Trypanosoma brucei*. *RNA* **17,** 1821–1830
21. Kaiser, P., and Wohlschlegel, J. (2005) Identification of ubiquitination sites and determination of ubiquitin-chain architectures by mass spectrometry. *Methods Enzymol.* **399,** 266–277
22. Wohlschlegel, J. A. (2009) Identification of SUMO-conjugated proteins and their SUMO attachment sites using proteomic mass spectrometry. *Methods Mol. Biol.* **497,** 33–49
23. Kelstrup, C. D., Young, C., Lavallee, R., Nielsen, M. L., and Olsen, J. V. (2012) Optimized fast and sensitive acquisition methods for shotgun proteomics on a quadrupole Orbitrap mass spectrometer. *J. Proteome Res.* **11,** 3487–3497
24. Michalski, A., Damoc, E., Hauschild, J. P., Lange, O., Wieghaus, A., Makarov, A., Nagaraj, N., Cox, J., Mann, M., and Horning, S. (2011) Mass spectrometry-based proteomics using Q Exactive, a high-performance benchtop quadrupole Orbitrap mass spectrometer. *Mol. Cell. Proteomics* **10,** M111.011015
25. Beausoleil, S. A., Villén, J., Gerber, S. A., Rush, J., and Gygi, S. P. (2006) A probability-based approach for high-throughput protein phosphorylation analysis and site localization. *Nat. Biotechnol.* **24,** 1285–1292
26. Cociorva, D., D, L. T., and Yates, J. R. (2007) Validation of tandem mass spectrometry database search results using DTASelect. *Curr. Protoc. Bioinformatics* Chapter 13, Unit 13.4
27. Tabb, D. L., McDonald, W. H., and Yates, J. R., 3rd. (2002) DTASelect and Contrast: tools for assembling and comparing protein identifications from shotgun proteomics. *J. Proteome Res.* **1,** 21–26
28. Xu, T., Venable, J. D., Park, S. K., Cociorva, D., Lu, B., Liao, L., Wohlschlegel, J., Hewel, J., and Yates III, J. R. (2006) ProLuCID: a fast and sensitive tandem mass spectra-based protein identification program. *Mol. Cell. Proteomics* **5,** S174
29. Elias, J. E., and Gygi, S. P. (2007) Target-decoy search strategy for increased confidence in large-scale protein identifications by mass spectrometry. *Nat. Methods* **4,** 207–214
30. Florens, L., Carozza, M. J., Swanson, S. K., Fournier, M., Coleman, M. K., Workman, J. L., and Washburn, M. P. (2006) Analyzing chromatin remodeling complexes using shotgun proteomics and normalized spectral abun-

dance factors. *Methods* **40,** 303–311
31. Panigrahi, A. K., Schnaufer, A., Carmean, N., Igo, R. P., Jr., Gygi, S. P., Ernst, N. L., Palazzo, S. S., Weston, D. S., Aebersold, R., Salavati, R., and Stuart, K. D. (2001) Four related proteins of the *Trypanosoma brucei* RNA editing complex. *Mol. Cell. Biol.* **21,** 6833–6840
32. Sabatini, R., and Hajduk, S. L. (1995) RNA ligase and its involvement in guide RNA/mRNA chimera formation: evidence for a cleavage-ligation mechanism of *Trypanosoma brucei* mRNA editing. *J. Biol. Chem.* **270,** 7233–7240
33. Ma, W. K., Cloutier, S. C., and Tran, E. J. (2013) The DEAD-box protein Dbp2 functions with the RNA-binding protein Yra1 to promote mRNP assembly. *J. Mol. Biol.* **425,** 3824–3838
34. Livak, K. J., and Schmittgen, T. D. (2001) Analysis of relative gene expression data using real-time quantitative PCR and the $2(-\Delta\Delta C(T))$ Method. *Methods* **25,** 402–408
35. Carnes, J., and Stuart, K. D. (2007) Uridine insertion/deletion editing activities. *Methods Enzymol.* **424,** 25–54
36. Marchler-Bauer, A., and Bryant, S. H. (2004) CD-Search: protein domain annotations on the fly. *Nucleic Acids Res.* **32,** W327–331
37. Kelley, L. A., and Sternberg, M. J. (2009) Protein structure prediction on the Web: a case study using the Phyre server. *Nat. Protoc.* **4,** 363–371
38. Rodrigues, J. P., Levitt, M., and Chopra, G. (2012) KoBaMIN: a knowledge-based minimization web server for protein structure refinement. *Nucleic Acids Res.* **40,** W323–328
39. Walbott, H., Mouffok, S., Capeyrou, R., Lebaron, S., Humbert, O., van Tilbeurgh, H., Henry, Y., and Leulliot, N. (2010) Prp43p contains a processive helicase structural architecture with a specific regulatory domain. *EMBO J.* **29,** 2194–2204
40. Segal, D. J., Crotty, J. W., Bhakta, M. S., Barbas, C. F., 3rd, and Horton, N. C. (2006) Structure of Aart, a designed six-finger zinc finger peptide, bound to DNA. *J. Mol. Biol.* **363,** 405–421
41. Moon, A. F., Mueller, G. A., Zhong, X., and Pedersen, L. C. (2010) A synergistic approach to protein crystallization: combination of a fixed-arm carrier with surface entropy reduction. *Protein Sci.* **19,** 901–913
42. Hashimi, H., Zíková, A., Panigrahi, A. K., Stuart, K. D., and Lukes, J. (2008) TbRGG1, an essential protein involved in kinetoplastid RNA metabolism that is associated with a novel multiprotein complex. *RNA* **14,** 970–980
43. Panigrahi, A. K., Zíková, A., Dalley, R. A., Acestor, N., Ogata, Y., Anupama, A., Myler, P. J., and Stuart, K. D. (2008) Mitochondrial complexes in *Trypanosoma brucei*: a novel complex and a unique oxidoreductase complex. *Mol. Cell. Proteomics* **7,** 534–545
44. Jarmoskaite, I., and Russell, R. (2014) RNA helicase proteins as chaperones and remodelers. *Annu. Rev. Biochem.* **83,** 697–725
45. Kruse, E., Voigt, C., Leeder, W. M., and Göringer, H. U. (2013) RNA helicases involved in U-insertion/deletion-type RNA editing. *Biochim. Biophys. Acta* **1829,** 835–841
46. Simpson, A. G., Stevens, J. R., and Lukes, J. (2006) The evolution and diversity of kinetoplastid flagellates. *Trends Parasitol.* **22,** 168–174
47. Masliah, G., Barraud, P., and Allain, F. H. (2013) RNA recognition by double-stranded RNA binding domains: a matter of shape and sequence. *Cell. Mol. Life Sci.* **70,** 1875–1895
48. Burge, R. G., Martinez-Yamout, M. A., Dyson, H. J., and Wright, P. E. (2014) Structural characterization of interactions between the double-stranded RNA-binding zinc finger protein JAZ and nucleic acids. *Biochemistry* **53,** 1495–1510
49. Robert-Paganin, J., Réty, S., and Leulliot, N. (2015) Regulation of DEAH/RHA helicases by G-patch proteins. *BioMed Res. Int.* **2015,** 931857
50. Künne, T., Swarts, D. C., and Brouns, S. J. (2014) Planting the seed: target recognition of short guide RNAs. *Trends Microbiol.* **22,** 74–83
51. Yang, M., May, W. S., and Ito, T. (1999) JAZ requires the double-stranded RNA-binding zinc finger motifs for nuclear localization. *J. Biol. Chem.* **274,** 27399–27406
52. Möller, H. M., Martinez-Yamout, M. A., Dyson, H. J., and Wright, P. E. (2005) Solution structure of the N-terminal zinc fingers of the *Xenopus laevis* double-stranded RNA-binding protein ZFa. *J. Mol. Biol.* **351,** 718–730